공학석사 학위논문

Effect of calcination temperature on Pd/ZSM-5 catalyst for selective catalytic reduction of NO_x by H_2

수소를 이용한 질소산화물 선택적 환원 반응에서 팔라듐/제올라이트 촉매의 소성 온도에 따른 영향

2023년 2월

서울대학교 대학원

화학생물공학부

문 세 이

Effect of calcination temperature on Pd/ZSM-5 catalyst for selective catalytic reduction of NO_x by H_2

지도 교수 김 도 희

이 논문을 공학석사 학위논문으로 제출함
2023년 1월

서울대학교 대학원
화학생물공학부
문 세 이

문세이의 공학석사 학위논문을 인준함
2023년 1월

위 원 장 이 원 보 (인)

부위원장 김 도 희 (인)

위 원 강 종 헌 (인)

Abstract

Nitrogen oxides (NO_x) are pollutants that have a harmful effect on the human body and the environment. NO_x emitted from automobile exhaust gas can be converted to clean N_2 through the selective catalytic reduction (SCR) reaction. NH_3-SCR is a widely used de-NO_x technology, but it has a disadvantage in that its activity is low in the low-temperature region. Also, secondary pollution is caused by ammonia slip, and additional costs are required to install the ammonia supplier. On the other hand, H_2-SCR is highly active in the low-temperature region. In addition, it does not generate secondary pollutants, so it is attracting attention as a technology that can compensate for the shortcomings of NH_3-SCR. As a catalyst utilized for H_2-SCR, a noble metal-based catalyst is typical, among which the Pd-based catalyst has high N_2 selectivity and resistance to CO poisoning.

In this study, the effect of calcination temperature on Pd/ZSM-5 catalysts for selective catalytic reduction of NO_x by H_2 (H_2-SCR) was investigated to improve low-temperature de-NO_x ability and N_2 selectivity. Pd/ZSM-5 catalysts were calcinated at different temperatures (e.g., 500, 650, 750, and 850 ℃) and treated at reductive conditions before the H_2-SCR reaction was performed. As a result, the calcination temperature at 750 ℃ resulted in the highest NO_x conversion and N_2 selectivity. Based on the H_2-O_2 reaction, the higher activity of Pd/ZSM-5 calcination at 750 ℃ was

attributed to the superior ability of H_2 activation for the H_2-SCR reaction. The combined X-ray diffraction (XRD), temperature-programmed hydride decomposition (TPHD), and transmission electron microscopy (TEM) data revealed that highly dispersed Pd particles were generated on the 750 ℃ calcination catalyst, while large Pd agglomerates were formed on the 500 ℃ calcination catalyst. In addition, the evolution of active intermediates such as bridging and chelating nitrates, NH_4^+ on Brønsted acid sites, and NH_3 on Lewis acid sites were analyzed by *in-situ* DRIFTS. Especially NH_4^+ species were found to be the most reactive intermediates which were known to contribute to the high activity and N_2 selectivity by participating in the NH_3-SCR reaction route. The catalytic activity of Pd/ZSM-5 is improved by optimizing the calcination temperature, resulting in high Pd dispersion. In addition, Pd 750 ℃ calcination catalyst showed high de-NO_x activity in the presence of CO, indicating it has a high potential for industrial applications because of its simple preparation method and high resistance to CO.

Keyword : Selective catalytic reduction; H_2-SCR reaction; Pd/ZSM-5 catalyst; calcination temperature; high dispersion

Student Number : 2021-20560

Table of Contents

Chapter 1. Introduction

1.1. Selective Catalytic Reduction (SCR) technology for reducing NO_x emissions

Nitrogen oxides (NO_x) have caused serious environmental problems such as photochemical smog, acid rain, and particulate matter which is harmful to the human respiratory system. To effectively address NO_x from the exhaust gas, many technologies such as selective catalytic reduction (SCR), passive NO_x adsorbers (PNA), and selective NO_x recirculation (SNR) are proposed and applied to proper pollutant sources [1-4]. SCR using ammonia as a reducing agent (NH_3-SCR) has been widely used to eliminate NO_x emitted from diesel engines, which operate under strongly oxidizing conditions. Despite the high performance of NH_3-SCR over a high-temperature range (>350 ℃), it has some problems such as secondary pollution from NH_3 slip or additional costs for the system to supply NH_3 or urea to the vehicle [5, 6]. In this situation, H_2 is proposed as an alternative reducing agent because H_2-SCR has high activity at a low-temperature range (<200 ℃) and this process produces no greenhouse gas or harmful gas at all. Moreover, no infrastructure for reductant storage and supply system is required because H_2 can be on-board generated via diesel fuel reforming [7]. Also, carbon-zero hydrogen combustion contributes to carbon neutrality. In this case, the fuel can be directly used as a reductant [8]. Furthermore, automobile exhaust gas contains CO, and diesel fuel reforming also produces

H_2 and CO together. CO can act as a catalytic poison that causes catalytic deactivation. Pt-based catalyst is susceptible to CO poisoning because of its strong adsorption to CO [9, 10] . However, it has been reported that Pd-based catalysts have relatively lower sensitivity to CO, so the catalytic activity of Pd-based catalysts can be less affected by the presence of CO [11]. For these reasons, Pd catalyst for the H_2-SCR reaction is gaining more attention due to its potential as effective and clean de-NO_x technology.

1.2. Pd/ZSM-5

In previous research, supported noble metal catalysts based on Pd or Pt have been investigated and regarded as the most effective H_2-SCR catalyst. Among these catalysts, Pd-based catalysts were found to show higher N_2 selectivity than Pt-based catalysts [12-14]. Various studies about Pd-based catalysts were performed on promoters, supports, catalyst preparation methods, and mechanism of the reaction. It was reported that 80 % of NO_x conversion at 150 ℃ was achieved by adding V_2O_5 to $Pd/TiO_2/Al_2O_3$ [15]. In addition to V_2O_5, Mn [16], Ni [17], and K_2O [18] were also used as promoters to enhance the de-NO_x activity of Pd-based catalysts. In the aspect of different supports, single oxide or various mixed oxide catalysts, and perovskite-like catalysts were studied for the low-temperature H_2-SCR reaction [19, 20]. B.Wen found that NO_x conversion and N_2 selectivity can be improved by using the sublimation method than using the ion-exchange method, in which

Pd/MFI achieved 70 % of NO_x conversion at 100 ℃ [21]. Several researchers investigated the mechanism of the H_2-SCR reaction on various catalysts and found that NH_4^+ ions are very active reaction intermediates. By using the in situ Diffuse Reflectance Infrared Fourier Transform Spectroscopy (DRIFTS), the appearance of the band of NH_4^+ is related to the higher catalytic activity [15, 22-24].

Various Pd species such as PdO, isolated Pd^{2+} ions, and metallic Pd on small-pore zeolite were found to have different reaction activities. For example, it is widely accepted that Pd^{2+} ions show significant catalytic activity on NO_x adsorption [25-27], while PdO clusters on zeolite are appropriate for the CH_4 combustion reactions [28]. For the H_2-SCR reaction, it is well recognized that Pd in a metallic state displays higher activity than PdO agglomerates or isolated Pd^{2+} ions [18, 21]. In a similar way, Pt in a metallic state is known as the primary active site of the H_2-SCR reaction [13, 29].

1.3. Objectives

In this study, various Pd catalysts supported on ZSM-5 were prepared by fixing the loading of Pd and the condition of reductive treatment, only varying the calcination temperatures. Atomically dispersed Pd^{2+} ions were generated by calcination at 750 ℃ [25], and small Pd^0 particles were formed by the subsequent reductive treatment to improve the catalytic activity of Pd/ZSM-5 for the H_2-SCR reaction. However, PdO agglomerates were

reduced to large Pd^0 particles in ZSM-5 after the calcination at 500 ℃ followed by reductive treatment. The influence of calcination temperature on the Pd particle size and activity of the H_2-SCR reaction was investigated by using various characterization methods. Not only the catalytic activity and N_2 selectivity were improved on the 750 ℃ calcination Pd/ZSM-5, but also the catalyst could be prepared simply by controlling the calcination temperature.

Chapter 2. Experimental

2.1. Catalyst preparation

All of the Pd-based catalysts used in this work were prepared according to the previous work of J.Lee [25]. Ammonium (NH_4)-ZSM-5 (Si/Al_2=23) was purchased from Alfa-Aesar and palladium(II) nitrate dihydrate ($Pd(NO_3)_2(H_2O)_2$) was purchased from Sigma-Aldrich. Parent NH_4-ZSM-5 was ion-exchanged with Pd precursor. 0.05 g of $Pd(NO_3)_2(H_2O)_2$ was dissolved in 100 ml of deionized water (DIW) and magnetically stirred at 400 rpm for 2 h. Subsequently, 2 g of NH_4-ZSM-5 was introduced to the solution. The mixed solution was transferred to a 65 ℃ water bath and magnetically stirred at 400 rpm for 24 h. The ion-exchanged zeolite was filtered with 1 L of the DIW, and dried at 105 ℃ in an oven for 6 h. The dried catalysts were calcinated for 2 h under a 100ml/min flow of 15 % O_2/N_2, and the catalysts were pelletized, crushed, and sieved. The calcinated catalyst was denoted as XC where X matches the calcination temperatures (X=500, 650, 750, or 850 ℃); for example, if 1-wt % of Pd was loaded on ZSM-5 and calcinated at 500 ℃, it was denoted as “Pd/Z_500C”. *In-situ* reductive treatment was carried out for all of the catalysts at the same condition; heated at 300 ℃ for 30 min under 4 % H_2/N_2. *In-situ* reductive treatment was performed before catalytic activity tests and catalyst characterization.

2.2. Catalyst characterization

The BET surface area and pore volume of the catalysts were obtained by applying Brunauer-Emmett-Teller (BET) methods to the nitrogen adsorption-desorption isotherms measured with BELSORP-mini II (BEL Japan) instrument at -196 ℃ of liquid nitrogen. Before the analysis, all of the catalysts were pretreated under vacuum condition at 250 ℃ for 4 h to remove remaining impurities. Inductively coupled plasma-atomic emission spectroscopy (ICP-AES) analysis with ICPS-8100 (Shimadzu) device was carried out to measure the Pd loadings of the catalysts. For this analysis, 40 mg of catalyst was dissolved in aqua regia, which is composed of a 3:1 molar mixture of hydrochloric acid and nitric acid. X-Ray diffraction (XRD) patterns of the catalysts were obtained from a powder X-Ray diffractometer (Smartlab, Rigaku). The X-Ray source was Cu-Kα radiation (λ = 0.1542 nm) operated at 40 kV and 50 mA. The overall XRD patterns were obtained from 5° to 80° at a scanning speed of 2.5°/min with a scanning-step size of 0.02°. Then, the same samples were fine-scanned from 37° to 43° at a scanning speed of 0.2°/min, in order to observe metallic Pd (Pd^0) peaks.

A temperature-programmed hydride decomposition (TPHD) was conducted with BEL-CAT-II (BEL Japan Inc.) analyzer to compare the metal dispersion of each catalyst qualitatively. 50 mg of samples were loaded in a quartz cell, pretreated under 5 % H_2/Ar for 30 min at 300 ℃, and purged with Ar for 30 min at 300 ℃. The sample was cooled down to -90 ℃, then the

temperature was raised from -90 ℃ to 400 ℃ at a rate of 10 ℃/min under 5 % H_2/Ar to collect TPHD profiles with thermal conductivity detector (TCD) by monitoring the hydrogen evolution in the process of β-hydride decomposition.

Transmission electron microscopy (TEM) image was obtained and energy-dispersive spectroscopy (EDS) mapping analysis was carried out at 200 kV in a JEM-ARM200F (Cold FEG) (JEOL Ltd.) electron microscope equipped with a field-emission gun in order to investigate the catalytic morphology and dispersion. Before the analysis, samples were suspended in methanol by sonication. The methanol medium was loaded dropwise onto carbon-deposited Cu grids and dried overnight at 65 ℃. To calculate the Pd dispersion of each sample and obtain the size distribution curves, metallic Pd particles were counted from TEM images with ImageJ software. Pd dispersion was calculated from size distribution curves by using the following equation [30]:

$$D\ (\%) = \frac{115.4}{d_p^{0.81}}$$

For the equation above, D means Pd dispersion (%) and d_p indicates average particle diameter.

Diffuse reflectance infrared Fourier transform spectroscopy (DRIFTS) spectra were obtained from Nicolet 6700 (Thermo Scientific) spectrometer attached with a mercury-cadmium-telluride (MCT) detector and a DRIFT cell (HARRIC praying mantis^{TM}). Samples were *in-situ* pretreated under a flow of 4 % H_2/N_2 (50 ml/min) at 300 ℃ for 30 min and purged with

50 ml/min of N_2 for 1 h. Spectra were acquired in the range of 4000-800 cm^{-1} with 64 scans at a resolution of 4 cm^{-1} and after the purging process, background spectra were collected. After these processes, the temperature was cooled down to 100 ℃ and the reaction gas mixture (500 ppm NO, 2 % H_2, 5 % O_2 with N_2 balance, total flow rate 50 ml/min) was fed to the Pd/Z_750C sample. For the study of shutting down H_2 gas from the reaction gas mixture, Pd/Z_750C sample was exposed to the reaction gas mixture for 60 min to ensure the reaction steady-state was reached and the DRIFT spectra were recorded for 60 min after switching the feed gas from the reaction gas mixture to 2000 ppm NO, 5 % O_2 balanced with N_2.

2.3. Catalytic activity measurement

The activity of Pd/ZSM-5 catalyst was measured by carrying out the de-NO_x reaction in the presence of H_2 in a packed bed reactor system. 100 mg of sieved catalysts (180-250 μm, 60-80 mesh) were loaded in a 1/2 inch diameter quartz tubular reactor. For *in-situ* reductive treatment, catalysts were heated to 300 ℃ for 30 min under 4 % H_2/N_2 flow. After the reductive treatment, the furnace temperature was cooled down to 25 ℃ while the reactor was purged under a flow of pure N_2. The reactant gas mixture consisted of 500 ppm NO, 2 % H_2, 5 % O_2, and 5 % H_2O in N_2 balance with a total flow rate of 200 ml/min (*GHSV* = 120,000 h^{-1}).

All of the data for measuring catalytic activity were acquired when

the reaction reached to a steady-state. During the experiment, a thermocouple was placed vertically inside the reactor and 3mm above the loaded catalyst sample to ensure precise control of the reaction temperature. Concentration data were collected from 7 points, from 100 ℃ to 300 ℃. The intervals of the temperature were 25 ℃ for 100 ℃ to 200 ℃ points, while those were 50 ℃ for 200 ℃ to 300 ℃ points, in order to focus on measuring catalytic activity at a low-temperature range. Severe temperature elevation and overshooting were hindered by fixing a ramping rate at 5 ℃/min. At each point, the reaction temperature was maintained for 70 min to ensure that the concentration of the outlet remained at the steady-state. The concentrations of NO, NO_2, N_2O, and NH_3 were quantified by using an online FT-IR spectrometer (Nicolet iS50, Thermo Scientific) equipped with an MCT detector and a 2 m gas cell. Every 60 seconds, the concentrations of NO, NO_2, N_2O, and NH_3 were analyzed from the acquired IR spectra. H_2 in the effluent gas was analyzed by using a thermal conductivity detector in a gas chromatograph.

Furthermore, NO_x conversion, H_2 conversion, and N_2 selectivity were calculated by following equations (Eqn (1)-(3)) and these values were used to indicate catalytic activity for the H_2-SCR reaction.

$$NO_x \text{ conversion } (\%) = \frac{[NO_x]_{in} - [NO_x]_{out}}{[NO_x]_{in}} \times 100\% \quad (1)$$

$$H_2 \text{ conversion } (\%) = \frac{[H_2]_{in} - [H_2]_{out}}{[H_2]_{in}} \times 100\% \quad (2)$$

$$N_2 \text{ selectivity } (\%) = \frac{[NO_x]_{in} - [NO_x]_{out} - 2[N_2O]_{out} - [NH_3]_{out}}{[NO_x]_{in} - [NO_x]_{out}} \times 100\% \quad (3)$$

In the equations above, $[NO_x]_{in}$ and $[NO_x]_{out}$ mean the concentration of nitrogen oxide plus nitrogen dioxide ($NO+NO_2$) of the inlet and outlet, respectively. Likewise, $[H_2]_{in}$, $[H_2]_{out}$, $[N_2O]_{out}$, and $[NH_3]_{out}$ represent the concentration of H_2, N_2O, and NH_3 at the inlet or outlet of the reactor.

Chapter 3. Results and discussion

3.1. Effect of calcination temperature on H_2-SCR performance

Fig. 1 presents the NO_x conversion and N_2 selectivity from 100 ℃ to 300 ℃ over 500, 650, 750, and 850℃ calcination Pd/ZSM-5 catalysts, respectively. NO_x conversion reached the maximum value of 96.7 % and N_2 selectivity achieved 96.8 % at 150 ℃ over the Pd/Z_750C catalyst while Pd/Z_500C catalyst showed only 86.7 % of NO_x conversion and 77.3 % of N_2 selectivity at the same temperature. For all catalysts, only N_2O was produced as a by-product, and no other products (e.g., NH_3 or NO_2) were produced except N_2O. Meanwhile, NO_x conversion started to decrease rapidly at 250 ℃ and plummeted to 40.1 % over Pd/Z_500C catalyst at 300 ℃. As the reaction temperature increases, the consumption of H_2 by O_2 is promoted so that the desired reduction of NO is inhibited by this side reaction [21, 31, 32].

As the calcination temperature increased from 500 ℃ to 750 ℃, overall catalytic activity increased. However, Pd/Z_850C catalyst showed 84.3 % of NO_x conversion at 150 ℃, which was lower than that of Pd/Z_750C. Pd/Z_750C showed slightly higher NO_x conversion and much higher N_2 selectivity compared with Pd/Z_650C at a low-temperature range. Thus, the order of the catalytic performance was 750C>650C>850C>500C considering

both NO_x conversion and N_2 selectivity. Therefore, Pd/Z_750C and Pd/Z_500C were selected to conduct the further investigation for the effect of calcination temperature on Pd species in the H_2-SCR reaction.

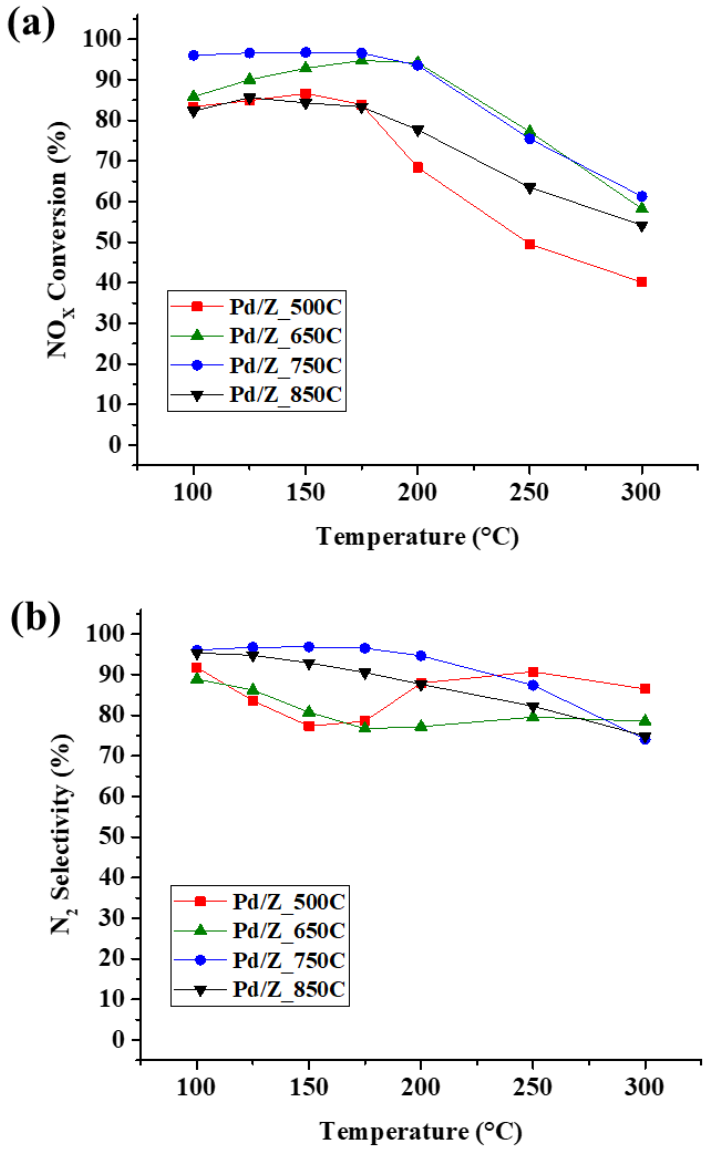

Fig. 1. H_2-SCR reaction performed on 500, 650, 750, and 850 ℃ calcination Pd/ZSM-5 catalysts. (a) NO_x conversion; (b) N_2 selectivity. Reaction conditions: 500 ppm NO, 2 % H_2, 5 % O_2, and 5 % H_2O balanced with N_2. *GHSV*=120,000 h^{-1}.

To compare the catalytic activity of Pd/Z_500C and Pd/Z_750C samples, H_2-O_2 reaction was performed as probe reaction. Several researchers investigated the difference in catalytic activity for the H_2-SCR reaction by comparing intrinsic reaction rates of H_2-O_2 reaction over different catalysts [14, 33, 34]. The promotional effect of W on the Pt-based catalyst was explained by the experiment that the Pt-W catalyst showed much higher activity than the Pt catalyst for the H_2-O_2 reaction. Pt presented a metallic state when W was doped to the catalyst so that the active Pt^0 promoted the H_2 activation [29].

Fig. 2(a) shows comparative results of the H_2 conversion of Pd/Z_500C and Pd/Z_750C for the H_2-O_2 reaction at 50-300 ℃ range. Pd/Z_750C achieved 100 % of H_2 conversion at 100 ℃, while Pd/Z_500C only reached 70.4 % of H_2 conversion at the same temperature. At 50-100 ℃ range, higher H_2 conversion was achieved over Pd/Z_750C than Pd/Z_500C sample, which indicates that the former is more active for the H_2 activation.

Similarly, another probe reaction of H_2-NO reaction is performed on Pd/Z_500C and Pd/Z_750C at 50-300 ℃ range and the result is presented in Fig. 2(b). Unlike the NO-H_2-O_2 reaction (H_2-SCR), the NO_x conversion increased as the reaction temperature increased at each sample, while Pd/Z_750C always showed higher NO_x conversion than Pd/Z_500C over every reaction temperature point. Although various reactions such as NO dissociation, H_2 activation, N_{ad}-H_{ad} reaction, or O_{ad}-H_{ad} reaction are

concerned in this condition, higher NO_x conversion in the H_2-NO reaction indicates that NO dissociation occurred more actively on Pd/Z_750C than Pd/Z_500C.

It was reported that the H_2 activation and NO dissociation step is crucial for the H_2-SCR reaction, because desirable N_2 can be produced only after the dissociation of H_2 and NO [35-38]. In addition, it has been reported that H_{ad} on metal assists the dissociation of NO so that the activated H atom promotes the N-O bond fission, leading to higher performance for the H_2-SCR reaction [34, 39, 40]. Therefore, it can be seen that Pd/Z_750C is more active than Pd/Z_500C for the H_2-SCR reaction as it presented higher activity for the H_2-O_2 reaction.

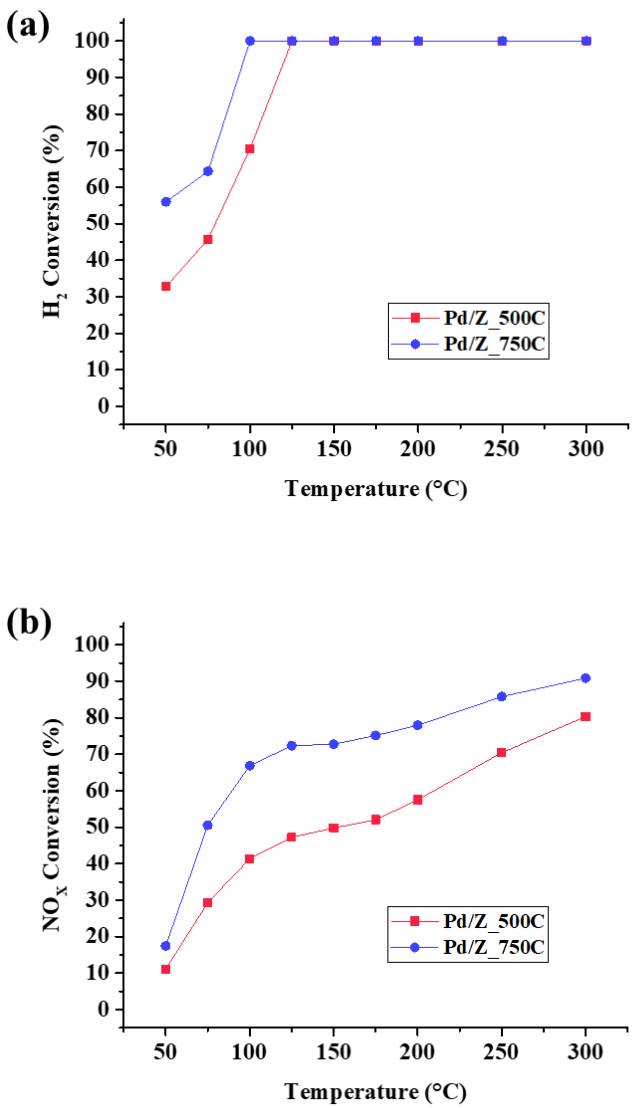

Fig. 2. (a) H_2 conversion over Pd/Z_500C(■) and Pd/Z_750C(●) for the H_2-O_2 reaction. Reaction conditions: 2000 ppm H_2, 5000 ppm O_2, and 5 % H_2O balanced with N_2. *GHSV*=4,800,000 h^{-1}. (b) NO_x conversion over Pd/Z_500C(■) and Pd/Z_750C(●) for the H_2-NO reaction. Reaction conditions: 500 ppm NO, 2 % H_2, and 5 % H_2O balanced with N_2. *GHSV*= 4,800,000 h^{-1}.

3.2. Catalyst characterization

To investigate the textural properties of the catalysts, actual Pd loading, BET surface area, and pore volume are listed in Table 1. Based on the ICP-AES analysis, all of the Pd precursors were successfully ion-exchanged regardless of the calcination temperature. The BET surface area and pore volume did not change much as the calcination temperature increased.

Likewise, from the XRD patterns ranging from 5° to 80° (Fig. 3(a)), characteristic ZSM-5 peaks appeared on all of the catalysts, with similar intensities. Considering the BET and XRD results, the zeolite structure was preserved after the loading of Pd, the calcination, and the reductive treatment. To observe peaks of Pd species, the region between 37° and 43° was finely scanned. In Fig. 3(b), the metallic Pd peak appeared at 40.3° only on the 500C sample. According to the previous work, Pd species are atomically dispersed as Pd^{2+} ions after the calcination at 750 ℃ under oxidative condition. However, it was reported that when Pd/ZSM-5 is calcinated at 500 ℃, the presence of bulk PdO species is supported by XRD and H_2-temperature programmed reduction (H_2-TPR) results [25]. Therefore, on the 500C catalyst followed by reductive treatment, bulk PdO was reduced to Pd^0 agglomerates which were large enough to be detected as characteristic Pd^0 peaks in XRD. When the calcination temperature was higher than 500 ℃, atomically dispersed Pd^{2+} ions were also reduced to Pd^0, but the particle size was too

small to be detectable in XRD. It could be seen that the 500C sample had larger Pd agglomerates and lower dispersion than other catalysts which were calcinated at higher temperatures.

Table 1

Pd content, Surface area, and pore volume of Pd/ZSM-5 catalysts

Catalyst	Pd content (wt%) [a]	Surface area (m^2/g) [b]	Pore volume (cm^3/g) [c]
ZSM-5_ 500C	-	360.1	0.25
Pd/Z_500C	0.98	352.1	0.24
Pd/Z_650C	1.04	344.5	0.24
Pd/Z_750C	1.04	340.8	0.23
Pd/Z_850C	1.03	349.3	0.26

[a] From ICP-AES

[b] Calculated by the BET equation at relative pressure (P/P_0) of 0.05-0.30

[c] Total pore volume at $P/P_0 \sim 0.99$

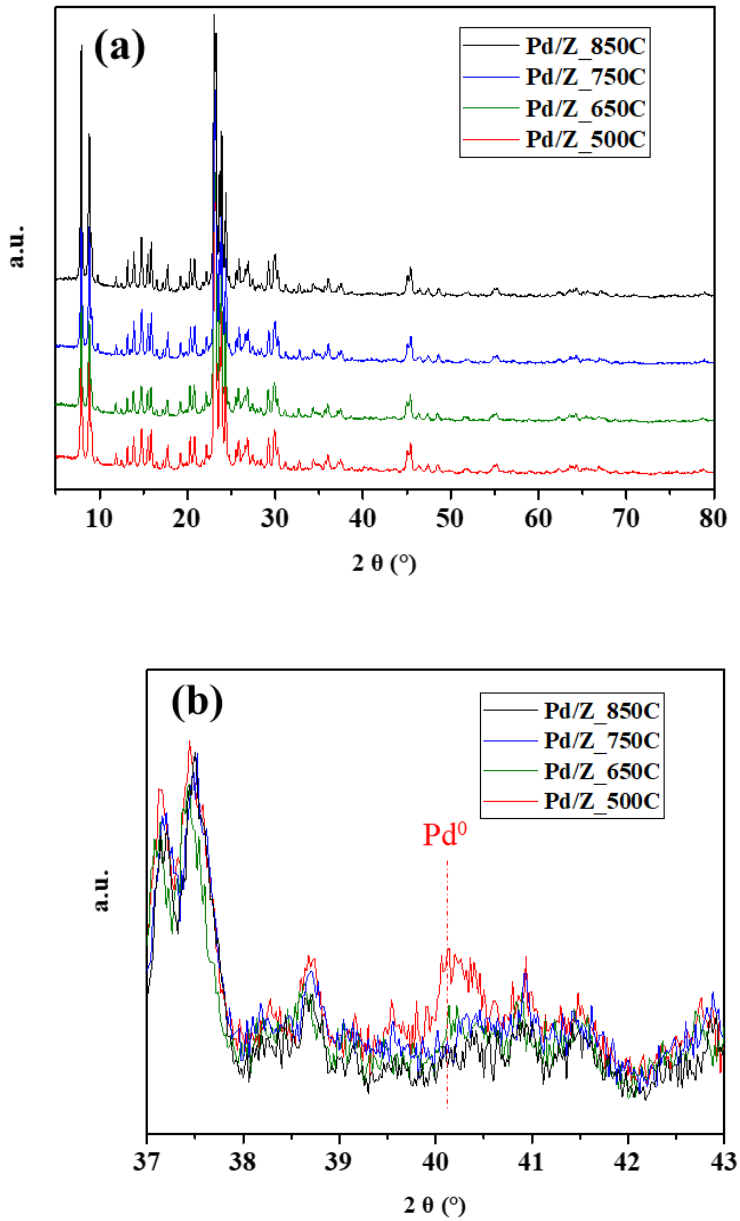

Fig. 3. XRD patterns of Pd/ZSM-5 catalysts with different calcination temperature. (a) scan over a wide range of 5-80° with a scan speed of 2.5°/min; (b) fine scan in a narrow range of 37-43° with a scan speed of 0.2°/min.

Temperature-programmed hydride decomposition (TPHD) analysis has been used as a qualitative tool for comparing the metal dispersion. In TPHD analysis, Pd hydride (PdH_x) species produced by the pre-treatment using H_2 decompose as the temperature increases. The decomposition of PdH_x species leads to the evolution of hydrogen gas, which is detected by TCD and displayed as a negative peak. Bonarowska et al. reported that when the catalysts are poorly dispersed, the negative peak in the TPHD curve was significantly amplified [41]. Similarly, Boudart et al. reported results that the solubility of hydrogen in Pd catalyst increases as the dispersion decreases [42]. In Fig. 4, the TPHD curves of Pd/Z_500C and Pd/Z_750C pre-treated under H_2 at 300℃ are presented. For a comparison, the TPHD profile of 1-wt% Pd/Al_2O_3_500C is also displayed. The peaks below 0 ℃ originated from the desorption physically adsorbed Ar from the zeolite [43]. Two PdH_x decomposition peaks were observed at 33 ℃ and 58 ℃ on Pd/Z_500C, while Pd/Z_750C showed a negligible negative peak. Thus, Pd/Z_750C had higher Pd dispersion than Pd/Z_500C, which was in agreement with the XRD data.

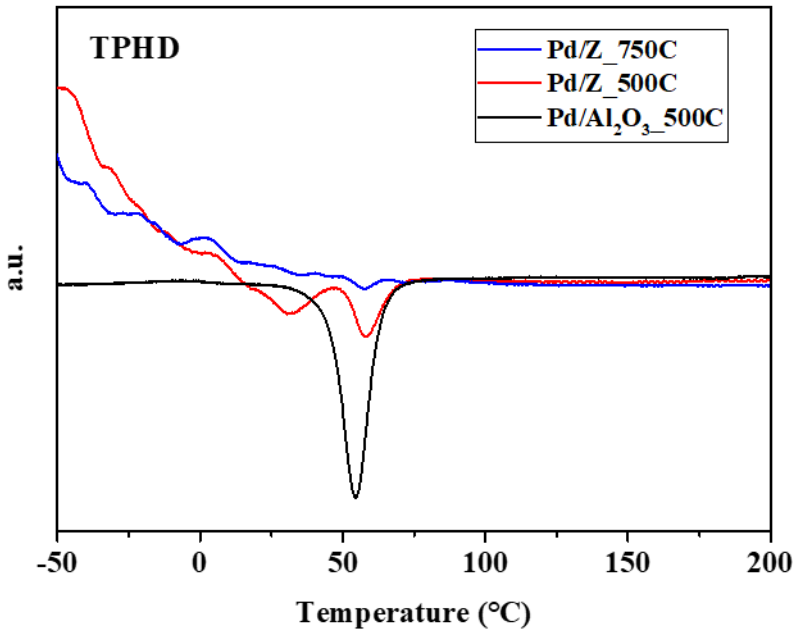

Fig. 4. TPHD curves of Pd/Z_500C and Pd/Z 750C samples. The catalysts were treated under 5 % H_2/Ar at 300 °C for 30 min and purged by Ar at 300 °C to remove impurities from samples. After the sample was cooled down to -90 °C, the temperature was ramped under flow of 5 % H_2/Ar.

Pd supported on zeolite tends to easily agglomerate when it is exposed to CO, even at the room temperature. In this case, CO chemisorption is not a proper method for the estimation of the Pd dispersion [26, 44]. For this reason, the Pd dispersion of each sample was calculated based on TEM images. According to the TEM image of the Pd/Z_500C (Fig. 5(a)), various sizes of Pd nanoparticles were observed, which ranged from 2nm to 22nm. However, on the Pd/Z_750C (Fig. 5(b)), there was no Pd nanoparticle observed that was larger than 3.1nm. Pd particle size distribution and average particle size were estimated from TEM images (Fig. 5(c) and Fig. 5(d)). Pd particles had uniform size and were well-dispersed on the 750C sample (Fig. 5(d)) than the 500C sample (Fig. 5(c)). The average size of Pd nanoparticles was measured as 7.8nm and 2.1nm on the Pd/Z_500C and the Pd/Z_750C sample, respectively. Moreover, the Pd dispersions were calculated based on the size distribution curve [30], which were 21.9% and 62.9% on the Pd/Z_500C and the Pd/Z_750C sample, respectively.

Combined XRD, TPHD data, and TEM results indicated that Pd nanoparticles had higher dispersion after the calcination at 750 ℃ followed by the reductive treatment than the calcination at 500 ℃ and the reductive treatment. Owing to the high-dispersed small Pd nanoparticles, it seems that more active sites exist on the 750C catalyst than on the 500C catalyst, which lead to superior H_2-SCR reaction activity.

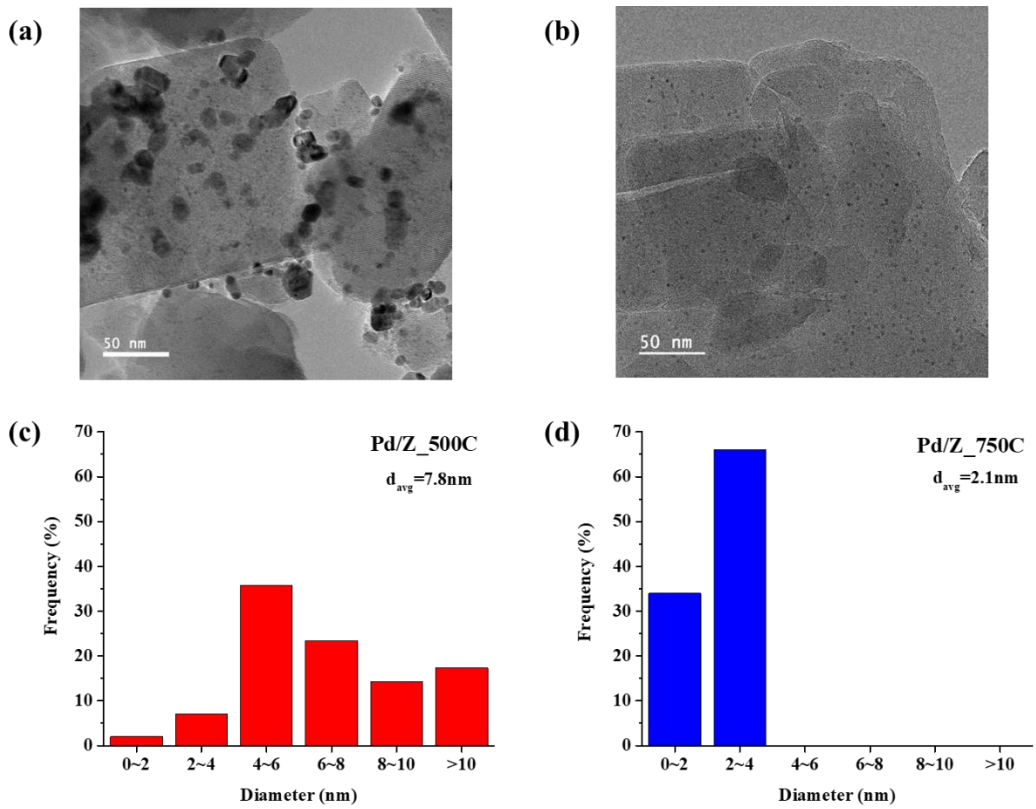

Fig. 5. TEM images of (a) Pd/Z_500C and (b) Pd/Z_750C catalysts. Histograms of the particle size distribution for (c) Pd/Z_500C and (d) Pd/Z_750C catalysts.

3.3. in situ DRIFTS study

3.3.1. Steady state reactions under $NO+O_2+H_2$

In Fig. 6, the changes of *in situ* DRIFT spectra of adsorbed species over the Pd/Z_750C catalyst at 100, 200, and 300 ℃ in the presence of $NO+O_2+H_2$ were displayed. The DRIFT spectra were obtained after 60 min to ensure that catalysts reached the reaction steady-state. Fig. 6 shows DRIFT spectra ranging between 1900-1100cm^{-1} under the reaction condition, which present various nitrogen-containing species adsorbed on the Pd/Z_750C catalyst. As reported in other research, two main species are involved in this reaction, such as NO_x adsorbed species and ammonia-related species. After flowing $NO+O_2+H_2$ gas to the Pd/Z_750C catalyst, various bands at 1726, 1690, 1626, 1465, 1320, and 1181cm^{-1} appeared, which were assigned to mono-nitrosyl on Pd^0 (1726 cm^{-1}) [45], bent Pd-NO species (1690 cm^{-1}) [16, 18], bridging nitrate (1626 cm^{-1}) [17, 46], NH_4^+ on Brønsted acid sites (1465 cm^{-1}) [15], chelating bidentate nitrate (1320 cm^{-1}) [45], and NH_3 on Lewis acid sites (1181 cm^{-1}) [15, 45]. It can be seen that bridging nitrate, NH_4^+ on Brønsted acid sites, and chelating bidentate nitrate are the main peaks highly active in this reaction because of their strong intensity compared with other bands. As the temperature increased to 300 ℃, the intensity of bridging nitrates decreased, which indicated that bridging nitrates were less active at the high temperature than other species adsorbed on the Pd/Z_750C catalyst.

However, other main peaks such as NH_4^+ on Brønsted acid sites did not vanish, indicating these species act as important reaction intermediates in the temperature range between 100 to 300 ℃.

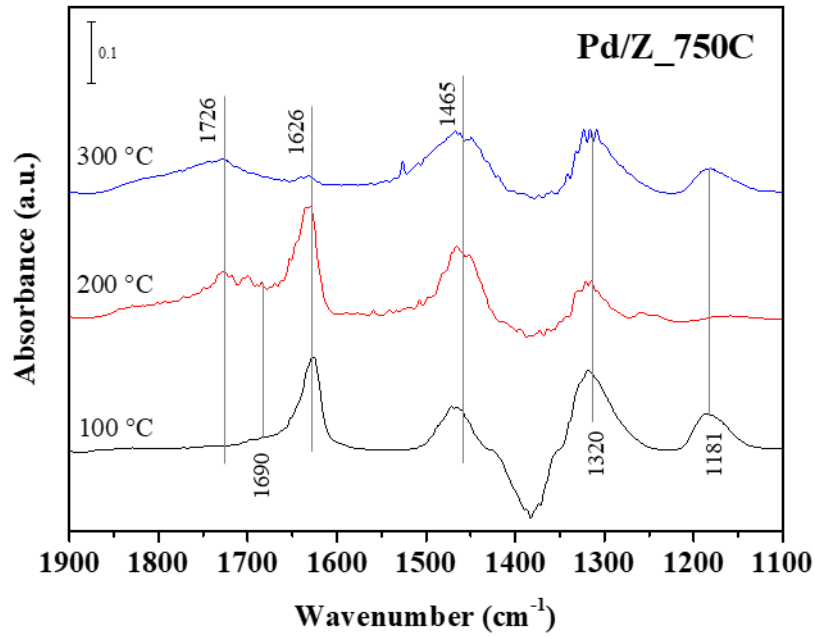

Fig. 6. In situ DRIFT spectra of surface species on the Pd/Z_750C catalyst at 100, 200, and 300 ℃ during the reaction. Reaction condition: 500 ppm NO, 5 % O_2, and 2 % H_2 balanced with N_2.

3.3.2. Switching gas from $NO+O_2+H_2$ to $NO+O_2$

Fig. 7 shows DRIFT spectra of Pd/Z_750C after switching gas flow from $NO+O_2+H_2$ (reaction condition) to $NO+O_2$ at 100 ℃. When H_2 was off, bands of bridging and chelating nitrate species (1626 and 1320 cm^{-1}) and bands related with ammonia species (1465 and 1181 cm^{-1}) gradually disappeared, while new bands at 1880 and 1832cm^{-1} which are assigned to NO adsorbed on Pd^{2+} ions appeared [47]. This indicates that metallic Pd^0 was oxidized to Pd^{2+} ions within 20 min when the feed gas was changed from $NO+O_2+H_2$ to $NO+O_2$. The bands at 1465 and 1181 cm^{-1} rapidly decreased and vanished within 20 min, indicating that *in-situ* generated NH_4^+ ions and NH_3 species were highly active species for the H_2-SCR reaction. Meanwhile, NO_x adsorbed species (the bands at 1626 and 1320 cm^{-1}) gradually decreased but did not completely vanish after 60 min of shuting off H_2 from the reaction feed gas. According to these results, *in-situ* generated NH_4^+ ions and NH_3 species were more active than bridging nitrate and chelating bidentate nitrate species. J.Shibata et al. proposed the mechanism that *in-situ* generated NH_4^+ ions on Brønsted acid sites react with $NO+O_2$ to produce more N_2, contributing to the higher NO_x conversion, N_2 selectivity, and wider operating window [22]. *In-situ* DRIFTS studies revealed that NH_4^+ ions are observed on the improved catalysts and these ammonia-related ions are more active than other nitrogen-containing species [15, 16]. Initially, dissociation of H_2

occurs on the metal surface and adsorbed NH_4^+ species are generated on Brønsted acid sites of ZSM-5. Then these ammonia-related ions attribute to the well-known NH_3-SCR reaction pathway that produces only N_2 and H_2O [23, 24, 38].

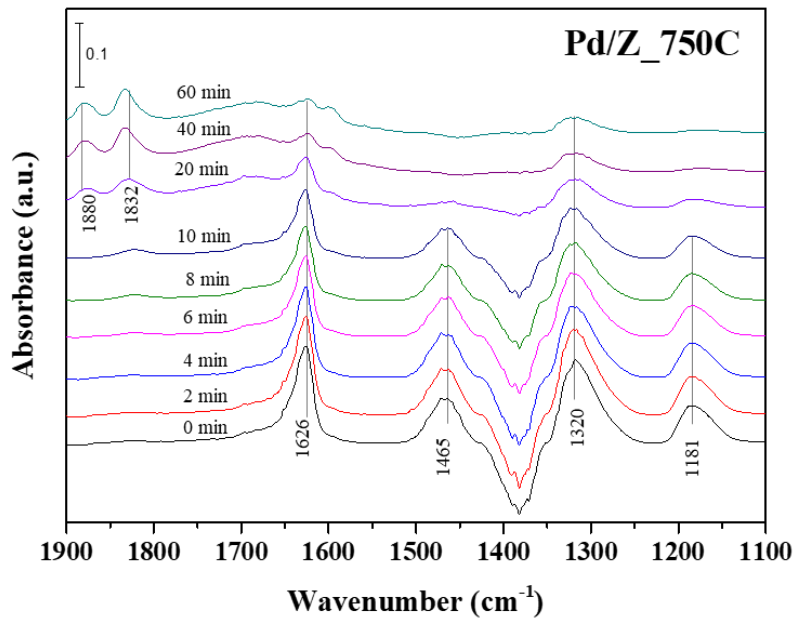

Fig. 7. In situ DRIFT spectra of surface species on the Pd/Z_750C catalyst at 100 ℃. The sample was exposed to $NO+O_2+H_2$ condition first, then the gas mixture was switched to $NO+O_2$. Condition: 500 ppm NO, 5 % O_2, and 2 % H_2 balanced with N_2 was switched to 500 ppm NO and 5 % O_2 balanced with N_2.

3.4. Effect of CO on the H_2-SCR reaction

To investigate the effect of CO on the H_2-SCR reaction, 0-5000 ppm CO was added to the feed gas and the catalytic activity of Pd/Z_750C was displayed in Fig. 8(a). The inclusion of CO up to 1000 ppm in the feed gas had a negligible effect on the NO_x conversion. Furthermore, the presence of 5000 ppm CO slightly decreased the NO_x conversion to 87 %, showing high resistance to CO.

For comparison, the effect of CO over Pt/ZSM-5 catalyst was displayed in Fig. 8(b). It has been reported that sintering of Pt occurred in Pt/ZSM-5 resulting from the calcination at high (> 500 ℃) temperatures [48, 49]. Therefore, 500 ℃ calcination Pt catalyst, instead of the same temperature as the Pd catalyst, was selected to minimize the influence of metal size on the H_2-SCR activity. Pt/Z_500C catalyst showed 61.4 % NO_x conversion when no CO was added to the feed gas. However, NO_x conversion decreased to 28.3 % on the Pt/Z catalyst under 1000 ppm CO, indicating severe deactivation of the catalyst via CO poisoning. On the other hand, the Pd/Z_750C catalyst was hardly affected by CO, maintaining >94% NO_x conversion under 1000 ppm CO.

Automobile exhaust gas contains CO, which can act as a catalytic poison that causes catalytic deactivation. However, Pd/Z_750C had lower sensitivity to CO, so that the H_2-SCR activity of Pd/Z_750C catalyst was

hardly affected by the presence of CO. These results indicate that Pd/Z_750C has a high potential for industrial application as an automobile exhaust purification catalyst.

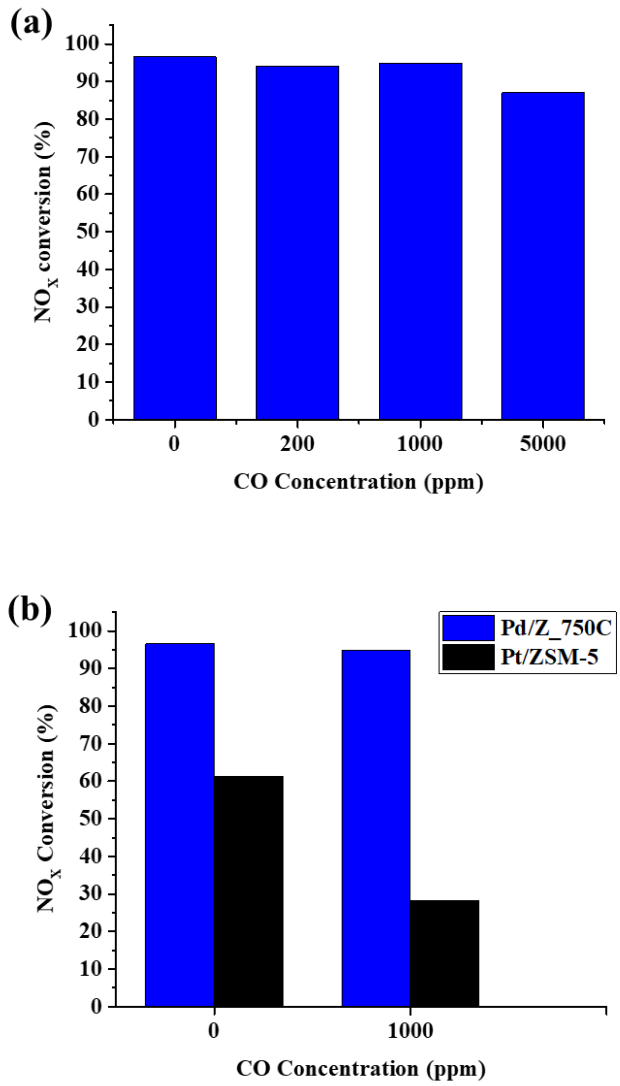

Fig. 8. (a) Effect of CO on the Pd/Z_750C catalyst for the H_2-SCR reaction performed at 175 ℃. Reaction conditions: 0-5000 ppm CO, 500 ppm NO, 2 % H_2, 5 % O_2, and 5 % H_2O balanced with N_2. *GHSV*=120,000 h^{-1}; (b) NO_x conversion of Pd and Pt-based catalyst in the presence of CO. Reaction conditions: 1000 ppm CO, 500 ppm NO, 2 % H_2, 5 % O_2, and 5 % H_2O balanced with N_2. *GHSV*=120,000 h^{-1}. Reaction temperature: 175 ℃.

Chapter 4. Summary and Conclusions

Pd/ZSM-5 catalyst calcinated at 750 ℃ (Pd/Z_750C) presented higher activity and N_2 selectivity for the de-NO_x reaction with H_2 in the presence of O_2 compared with Pd/ZSM-5 catalysts treated at 500, 650, or 850 ℃. There was no significant difference in BET surface area or pore volume between these catalysts, but the XRD patterns revealed that Pd/Z_750C showed no peaks of Pd^0 while Pd/Z_500C had Pd^0 peaks at 40°, indicating that Pd/Z_750C was highly dispersed than Pd/Z_500C. According to the TPHD data, Pd/Z_750C displayed negligible hydride decomposition peak, so it was well-dispersed and had no large Pd^0 agglomerates. TEM images were taken to estimate the Pd size distribution and dispersion, which were found to be 21.9 % for Pd/Z_500C and 62.9 % for Pd/Z_750C, respectively. The DRIFT spectra indicated that active reaction intermediates such as bridging nitrate, chelating bidentate nitrate, NH_4^+ on Brønsted acid sites, and NH_3 on Lewis acid sites were observed when the reaction gas mixture was fed to the Pd/Z_750C catalyst. Moreover, according to the DRIFT spectra obtained by switching feed gas from $NO+O_2+H_2$ to $NO+O_2$, NH_4^+ ions were highly active intermediates that contributed to the higher catalytic activity and N_2 selectivity of the Pd/Z_750C catalyst. In addition, the effect of CO on the Pd/Z_750C was also investigated. Pd/Z_750C displayed >94 % NO_x conversion even in the presence of 1000 ppm CO, indicating high resistance to CO compared with Pt-based catalyst. In

conclusion, Pd/Z_750C showed a potential for industrial application because it achieved high NO_x conversion, N_2 selectivity, and resistance to CO by optimizing the calcination temperature.

Bibliography

[1] Z. Liu, J. Li, S.I. Woo, Energy & Environmental Science, 5 (2012) 8799-8814.

[2] Z. Liu, J. Hao, L. Fu, T. Zhu, Applied Catalysis B: Environmental, 44 (2003) 355-370.

[3] Y. Gu, W.S. Epling, Applied Catalysis A: General, 570 (2019) 1-14.

[4] S. Hodjati, K. Vaezzadeh, C. Petit, V. Pitchon, A. Kiennemann, Catalysis Today, 59 (2000) 323-334.

[5] F. Nakajima, I. Hamada, Catalysis Today, 29 (1996) 109-115.

[6] L. Han, S. Cai, M. Gao, J.-y. Hasegawa, P. Wang, J. Zhang, L. Shi, D. Zhang, Chemical Reviews, 119 (2019) 10916-10976.

[7] S. Bensaid, E.M. Borla, N. Russo, D. Fino, V. Specchia, Industrial & Engineering Chemistry Research, 49 (2010) 10323-10333.

[8] M. Borchers, K. Keller, P. Lott, O. Deutschmann, Industrial & Engineering Chemistry Research, 60 (2021) 6613-6626.

[9] K. Yokota, M. Fukui, T. Tanaka, Applied Surface Science, 121-122 (1997) 273-277.

[10] J. Liu, F.R. Lucci, M. Yang, S. Lee, M.D. Marcinkowski, A.J. Therrien, C.T. Williams, E.C.H. Sykes, M. Flytzani-Stephanopoulos, Journal of the American Chemical Society, 138 (2016) 6396-6399.

[11] N. Macleod, R. Cropley, J.M. Keel, R.M. Lambert, Journal of Catalysis, 221 (2004) 20-31.

[12] Q. Yu, M. Richter, F. Kong, L. Li, G. Wu, N. Guan, Catalysis Today, 158 (2010) 452-458.

[13] M. Machida, S. Ikeda, D. Kurogi, T. Kijima, Applied Catalysis B: Environmental, 35 (2001) 107-116.

[14] A. Ueda, T. Nakao, M. Azuma, T. Kobayashi, Catalysis Today, 45 (1998) 135-138.

[15] G. Qi, R.T. Yang, F.C. Rinaldi, Journal of Catalysis, 237 (2006) 381-392.

[16] K. Duan, B. Chen, T. Zhu, Z. Liu, Applied Catalysis B: Environmental, 176-177 (2015) 618-626.

[17] Z. Hu, X. Yong, D. Li, R.T. Yang, Journal of Catalysis, 381 (2020) 204-214.

[18] L. Li, F. Zhang, N. Guan, E. Schreier, M. Richter, Catalysis Communications, 9 (2008) 1827-1832.

[19] G.L. Chiarello, D. Ferri, J.-D. Grunwaldt, L. Forni, A. Baiker, Journal of Catalysis, 252 (2007) 137-147.

[20] V.K. Patel, S. Sharma, Catalysis Today, 375 (2021) 591-600.

[21] B. Wen, Fuel, 81 (2002) 1841-1846.

[22] J. Shibata, M. Hashimoto, K.-i. Shimizu, H. Yoshida, T. Hattori, A. Satsuma, The Journal of Physical Chemistry B, 108 (2004) 18327-18335.

[23] S.M. Park, M.-Y. Kim, E.S. Kim, H.-S. Han, G. Seo, Applied Catalysis A: General, 395 (2011) 120-128.

[24] J.-B. Yang, O.-Z. Fu, D.-Y. Wu, S.-D. Wang, Applied Catalysis B: Environmental, 49 (2004) 61-65.

[25] J. Lee, Y. Ryou, S.J. Cho, H. Lee, C.H. Kim, D.H. Kim, Applied Catalysis B: Environmental, 226 (2018) 71-82.

[26] J. Lee, J. Kim, Y. Kim, S. Hwang, H. Lee, C.H. Kim, D.H. Kim, Applied Catalysis B: Environmental, 277 (2020) 119190.

[27] Y. Ryou, J. Lee, Y. Kim, S. Hwang, H. Lee, C.H. Kim, D.H. Kim, Applied Catalysis A: General, 569 (2019) 28-34.

[28] Y. Kim, J. Sung, S. Kang, J. Lee, M.-H. Kang, S. Hwang, H. Park, J. Kim, Y. Kim, E. Lee, G.-S. Park, D.H. Kim, J. Park, Journal of Materials Chemistry A, 9 (2021) 19796-19806.

[29] X. Zhang, X. Wang, X. Zhao, Y. Xu, Y. Liu, Q. Yu, Chemical Engineering Journal, 260 (2015) 419-426.

[30] A. Borodziński, M. Bonarowska, Langmuir, 13 (1997) 5613-5620.

[31] C.N. Costa, P.G. Savva, J.L.G. Fierro, A.M. Efstathiou, Applied Catalysis B: Environmental, 75 (2007) 147-156.

[32] M. Machida, S. Ikeda, Journal of Catalysis, 227 (2004) 53-59.

[33] C.N. Costa, A.M. Efstathiou, Applied Catalysis B: Environmental, 72 (2007) 240-252.

[34] B. Frank, G. Emig, A. Renken, Applied Catalysis B: Environmental, 19 (1998) 45-57.

[35] M. Machida, D. Kurogi, T. Kijima, The Journal of Physical Chemistry

B, 107 (2003) 196-202.

[36] C.N. Costa, A.M. Efstathiou, The Journal of Physical Chemistry B, 108 (2004) 2620-2630.

[37] R. Burch, A.A. Shestov, J.A. Sullivan, Journal of Catalysis, 188 (1999) 69-82.

[38] P. Wu, L. Li, Q. Yu, G. Wu, N. Guan, Catalysis Today, 158 (2010) 228-234.

[39] T.M. Salama, R. Ohnishi, T. Shido, M. Ichikawa, Journal of Catalysis, 162 (1996) 169-178.

[40] M. Uchida, A.T. Bell, Journal of Catalysis, 60 (1979) 204-215.

[41] M. Bonarowska, J. Pielaszek, W. Juszczyk, Z. Karpiński, Journal of Catalysis, 195 (2000) 304-315.

[42] M. Boudart, H.S. Hwang, Journal of Catalysis, 39 (1975) 44-52.

[43] B.J. Adelman, W.M.H. Sachtler, Applied Catalysis B: Environmental, 14 (1997) 1-11.

[44] L.L. Sheu, H. Knözinger, W.M.H. Sachtler, Catalysis Letters, 2 (1989) 129-137.

[45] J. Li, G. Wu, N. Guan, L. Li, Catalysis Communications, 24 (2012) 38-43.

[46] N. Macleod, R. Cropley, R.M. Lambert, Catalysis Letters, 86 (2003) 69-75.

[47] A.W. Aylor, L.J. Lobree, J.A. Reimer, A.T. Bell, Journal of Catalysis,

172 (1997) 453-462.

[48] J.E. Park, K.B. Kim, Y.-A. Kim, K.S. Song, E.D. Park, Catalysis Letters, 143 (2013) 1132-1138.

[49] G.N. Folefoc, J. Dwyer, Journal of Catalysis, 136 (1992) 43-49.

국 문 초 록

질소산화물(NO_x)은 인체와 환경에 해로운 영향을 끼치는 오염물질이다. 자동차 배기가스에서 배출된 질소산화물은 선택적 촉매환원(SCR) 반응을 통해 깨끗한 질소 기체로 전환될 수 있다. 암모니아-SCR은 널리 활용되는 질소산화물 저감 기술이나, 저온 영역에서 활성이 낮다는 단점을 가지고 있다. 또한, 암모니아 슬립으로 인한 2차 오염과 암모니아 공급 장치를 설치하기 위한 추가 비용이 발생한다는 단점이 있다. 반면, 수소-SCR은 저온 영역에서 활성이 매우 높아 암모니아-SCR의 단점을 보완할 수 있는 기술로서 주목받고 있다. 수소-SCR에 활용되는 촉매로는 귀금속 기반 촉매가 보편적이며, 특히 팔라듐(Pd) 기반 촉매는 높은 질소 선택도와 일산화탄소 피독 저항성을 가진다.

본 연구는 저온 영역에서의 질소산화물 저감 능력과 질소 선택도 향상을 위해 수소-SCR 반응에 적용된 Pd/ZSM-5 촉매의 소성 온도에 따른 영향을 다루었다. Pd/ZSM-5 촉매는 각각 500, 650, 750, 그리고 850℃에서 소성하였고 수소-SCR 반응에 앞서 환원 처리하였다. 결과적으로, 750℃ 소성 촉매가 가장 높은 질소산화물 전환율과 질소 선택도를 달성했다. 수소-산소 반응에 따르

면, 750℃ 촉매의 우수한 활성은 수소-SCR 반응에 필수적인 수소를 활성화하는 능력에서 기인한 것으로 보인다. X-선 회절분석(X-ray diffraction), 승온 수소화물 분해분석(temperature-programmed hydride decomposition), 투과전자현미경(transmission electron microscopy) 결과를 바탕으로 750℃ 소성 촉매에서 고분산된 팔라듐 입자가 형성된 반면, 500℃ 소성 촉매에서는 응집된 팔라듐 입자가 형성되었음을 밝혔다. 더 나아가, In-situ DRIFTS(Diffuse Reflection Infrared Spectroscopy) 기법을 통해 반응에 활발하게 참여하는 중간체들(다양한 구조의 질산염, 브뢴스테드 산점에 결합한 암모늄 이온, 루이스 산점에 결합한 암모니아 등)을 관찰하였다. 특히, 암모늄 이온은 암모니아-SCR 반응 경로에 참여하여 높은 활성과 질소 선택도에 기여하는 것으로 알려져 있을 뿐만 아니라, 본 반응에서도 가장 활발히 반응에 참여하는 중간체로 밝혀졌다. 또한, 750℃ 소성 촉매는 반응 조건에 일산화탄소가 포함되어도 여전히 높은 반응 활성을 유지하였다. 결론적으로, 750℃ 소성 Pd/ZSM-5 촉매는 단순한 제조 방법, 높은 수소-SCR 반응 활성, 일산화탄소 피독 저항성으로 인해 실제 공업 현장에서 활용할 수 있는 특성을 가지고 있다.

주요어: 선택적 촉매 환원; 수소-SCR 반응; Pd/ZSM-5; 소성 온도; 고분산
학번: 2021-20560